

SARS-Associated Viral Hepatitis Caused by a Novel Coronavirus: Report of Three Cases

Tai-Nin Chau,¹ Kam-Cheong Lee,¹ Hung Yao,¹ Tak-Yin Tsang,¹ Tat-Chong Chow,¹ Yiu-Cheong Yeung,¹ Kin-Wing Choi,¹ Yuk-Keung Tso,¹ Terence Lau,² Sik-To Lai,¹ and Ching-Lung Lai³

Liver impairment is commonly reported in up to 60% of patients who suffer from severe acute respiratory syndrome (SARS). Here we report the clinical course and liver pathology in three SARS patients with liver impairment. Three patients who fulfilled the World Health Organization case definition of probable SARS and developed marked elevation of alanine aminotransferase were included. Percutaneous liver biopsies were performed. Liver specimens were examined by light and electron microscopy, and immunohistochemistry. Reverse-transcriptase polymerase chain reaction (RT-PCR) using enhanced real-time PCR was applied to look for evidence of SARS-associated coronavirus infection. Marked accumulation of cells in mitosis was observed in two patients and apoptosis was observed in all three patients. Other common pathologic features included ballooning of hepatocytes and mild to moderate lobular lymphocytic infiltration. No eosinophilic infiltration, granuloma, cholestasis, fibrosis, or fibrin deposition was noted. Immunohistochemical studies revealed 0.5% to 11.4% of nuclei were positive for proliferative antigen Ki-67. RT-PCR showed evidence of SARS-associated coronavirus in the liver tissues, but not in the sera of all 3 patients. However, electron microscopy could not identify viral particles. No giant mitochondria, micro- or macro-vesicular steatosis was observed. In conclusion, hepatic impairment in patients with SARS is due to SARS-associated coronavirus infection of the liver. The prominence of mitotic activity of hepatocytes is unique and may be due to a hyperproliferative state with or without disruption of cell cycle by the coronavirus. With better knowledge of pathogenesis, specific therapy may be targeted to reduce viral replication and modify the disease course. (HEPATOLOGY 2004;39:302–310.)

Coronaviruses are enveloped viruses with single-stranded, positive-sense RNA that is 5' capped and 3' polyadenylated and replicates in the cytoplasm of infected cells.¹ They include a large number of viruses that infect different animal species. The predominant diseases associated with these viruses are respiratory and enteric infections, although hepatic and neurologic diseases also occur. Severe acute respiratory syndrome-associated coronavirus

(SARS-CoV) is a novel virus that has been found to be a causative agent of a recently described atypical pneumonia.^{2,3} The disease may progress rapidly, resulting in acute respiratory distress syndrome. At the time of writing, more than 8,221 individuals were affected worldwide and 735 patients had succumbed to the illness, which the World Health Organization (WHO) has termed *severe acute respiratory syndrome* (SARS).

Liver impairment is common and has been reported in up to 60% of patients suffering from SARS.^{2,4,5} The majority of these patients have been treated with antibiotics, antiviral medications, and steroids, which are potentially hepatotoxic. Hence, whether or not SARS-CoV infection can lead to liver damage *per se* remains unknown. Here we report the clinical course and liver pathology in three SARS patients with liver impairment.

Methods

Patients

Three patients who fulfilled the WHO case definition of probable SARS⁶ and developed liver derangement were

Abbreviations: SARS, severe acute respiratory syndrome; WHO, World Health Organization; RT-PCR, reverse-transcriptase polymerase chain reaction; PCR, polymerase chain reaction; SARS-CoV, SARS-associated coronavirus; CMV, cytomegalovirus; ALT, alanine aminotransferase.

From the ¹Department of Medicine and Geriatrics and Department of Pathology, Princess Margaret Hospital; ²Hong Kong DNA Chips Ltd.; and ³Department of Medicine, Queen Mary Hospital, University of Hong Kong, Hong Kong, China.

Received July 20, 2003; accepted November 19, 2003.

Address reprint requests to: Tai-Nin Chau, Department of Medicine and Geriatrics, Princess Margaret Hospital, Princess Margaret Hospital Road, Lai Chi Kok, Hong Kong SAR, China. E-mail: chautainin@hotmail.com; fax: +852-29903333.

Copyright © 2004 by the American Association for the Study of Liver Diseases.

Published online in Wiley InterScience (www.interscience.wiley.com).

DOI 10.1002/hep.20111

included in the study. Briefly, the case definition was: fever of 38° C or higher, cough or difficulty breathing, radiographic evidence of infiltrates consistent with pneumonia or respiratory distress syndrome, and either a history of exposure to a patient with SARS or a lack of response to empirical antimicrobial coverage for typical and atypical pneumonia. After informed consent was obtained from each patient, percutaneous liver biopsy was performed to look for the cause of elevated liver enzymes. Common causes of hepatitis were excluded by serologic tests, including anti-hepatitis A virus IgM antibodies, anti-hepatitis B core IgM, hepatitis B surface antigen, anti-hepatitis C antibody, and cytomegalovirus pp65 antigen. Abdominal ultrasonography was performed to rule out space-occupying lesions and biliary tract diseases. All patients received antimicrobial coverage for community-acquired pneumonia with ceftriaxone and clarithromycin or levofloxacin alone. Combination therapy using oral ribavirin 600 mg twice daily and Kaletra (lopinavir/ritonavir, Abbott Laboratories, North Chicago, IL) 1000 mg daily were commenced when patients did not respond to antibiotics within 48 hours. Kaletra is a co-formulation of two protease inhibitors: lopinavir and ritonavir. It is an experimental drug for coronavirus that depends on protease for cleavage of polypeptides and formation of viral structure. Methylprednisolone, given in three pulses at a dose of 500 mg to 1000 mg daily, was offered to patients who had persistent fever, radiologic progression of lung infiltrates, or signs of respiratory distress despite antiviral therapy.

Investigations

In addition to the aforementioned tests for viral hepatitis, routine microbiological investigations included blood, urine, and sputum culture for bacterial pathogens. The acute and convalescent sera were tested in parallel for SARS-associated coronavirus immunoglobulin G, with SARS-CoV-infected Vero cells fixed in acetone in an indirect immunofluorescent format.⁷ Reverse-transcriptase polymerase chain reaction (RT-PCR) for coronavirus was done on nasal and throat swabs, stool specimens, and liver tissues of patients.

Cores of 10- to 15-mm-long liver tissue were sent fresh to the histopathology laboratory for processing. Two 1-mm tissue fragments were fixed in 2.5% glutaraldehyde for transmission electron microscopy examination. A 5-mm-long tissue was immediately kept frozen at -70° C for molecular study. The remaining core of tissue was fixed in 10% neutral buffered formalin. The paraffin-embedded blocks of liver tissues were sectioned at 4 μ m for light microscopy. A panel of stains including hematoxylin and eosin, diastase periodic acid-schiff, Perls, Gor-

don and Sweets' reticulin, and Orcein were performed. The number of mitoses was counted in 1000 hepatocytes in each specimen, and the mitotic index was expressed as the percentage. Immunohistochemical study for Ki-67 antigen (DAKO rabbit antihuman Ki-67 antigen, code no. A047) was performed using the BIOTEK TM500-220 automated immunohistochemical stainer (DAKO, CA, USA). Ki-67 is a human nuclear antigen that is expressed during G1, S, G2, and M phases of the cell cycle but is absent in the quiescent G0 phase.⁸ Proliferating hepatocytes were identified by immunohistochemical staining of Ki-67. Only hepatocytes with distinct and near-total nuclear staining were considered positive. One thousand hepatocytes were counted in each specimen. The Ki-67 index was expressed as percentage of hepatocyte nuclei that showed positive staining pattern. Immunostaining for cytomegalovirus (CMV) using monoclonal mouse anti-cytomegalovirus antibodies (DAKO-CMV DDG9, CCH2, code no. M854) was also performed to exclude CMV infection.

Enhanced Real-Time PCR

Total RNA from samples was collected using a QIAamp Viral RNA Mini Kit (Qiagen, Hilden, Germany) according to the manufacturer's instructions. RNA was converted to cDNA using SuperScript II RNase H⁻ Reverse Transcriptase (Invitrogen Inc., CA, USA) according to the manufacturer's instructions, except that 300-ng random hexamer primers were used in place of oligo (dT)₁₂₋₁₈, and nuclease-free water was used in place of RNaseOUT Recombinant Ribonuclease Inhibitor (Invitrogen Inc., CA, USA). The new assay comprised a first round of conventional PCR followed by Taqman real-time fluorescent PCR (Eurogenetic Group, Belgium).⁹

First-round conventional PCR was as follows: in a total volume of 25 μ L, the following components were mixed: nuclease-free water (19.2 μ L), 0.2 mM dNTPs, 1U Platinum *Taq* DNA polymerase (Invitrogen), 5 mM MgCl₂, 1 \times PCR buffer, primers (10 μ M, 0.5 μ L each), and cDNA template (\approx 100 ng, 1 μ L). The PCR amplification was performed in a MasterCycler (Eppendorf, Hamburg, Germany) with the following temperature profile: DNA polymerase activation (95° C, 3 minutes); 10 cycles of denaturation (95° C, 10 seconds); annealing (60° C, 10 seconds); 1° C reduction after each cycle and extension (72° C, 20 seconds); 40 cycles of denaturation (95° C, 10 seconds); annealing (56° C, 10 seconds); and extension (72° C, 20 seconds). A variety of primers for conventional PCR were compared; their sequences are listed in Table 1.

Taqman real-time fluorescent PCR consisted of the following: in a total volume of 25 μ L, the following components were mixed: nuclease-free water (9.9 μ L), PCR

Table 1. Primers and Probes Used in This Study

Name	Origin	Assay, Orientation	Sequence (5'-3')	Coordinates*
Primer C	This study	Real-time PCR, antisense	AGT TGC ATG ACA GCC CTC TAC A	18260-18245
Primer D	This study	Real-time PCR, sense	CCC GCG AAG AAG CTA TTC G	18193-18211
Probe E	This study	Real-time PCR, fluorescent probe	CGT TCG TGC GTG GAT TGG CTT TG	18215-18237
SAR1S	CDC†	Conventional PCR, sense	CCT CTC TTG TTC TTG CTC GCA	15291-15271
SAR1As	CDC†	Conventional PCR, antisense	TAT AGT GAG CCG CCA CAC ATG	15371-15391
COR1	GVU‡	Conventional PCR, sense	CAC CGT TTC TAC AGG TTA GCT AAC GA	15318-15343
COR2	GVU‡	Conventional PCR, antisense	AAA TGT TTA CGC AGG TAA GCG TAA AA	15628-15603
BNIoutS2	BNI§	Conventional PCR, sense	ATG AAT TAC CAA GTC AAT GGT TAC	18153-18176
BNIoutAs	BNI§	Conventional PCR, antisense	CAT AAC CAG TCG GTA CAG CTA C	18342-18321

*Tor2 (GenBank # AY274119).

†Centers for Disease Control and Prevention, Atlanta, GA, USA.

‡Government Virus Unit, Hong Kong SAR, China.

§Bernard-Nocht Institute for Tropical Medicine, Hamburg, Germany.

mastermix (dNTPs, dUTP, HotStart *Taq* DNA polymerase, MgCl₂, uracil-N-glycosylase, and passive reference; 12.5 μL), primer C (5 μM, 1.0 μL), primer D (5 μM, 1.0 μL), probe E (10 μM, 2.6 μL), and amplified DNA template (≈100 ng, 1 μL). The 40 cycles of amplification were performed in an ABI Prism 7700 Sequence Detector (Applied Biosystems, CA, USA) with the following temperature profile: initial incubation (50° C, 2 minutes); DNA polymerase activation (95° C, 10 minutes); denaturation (95° C, 15 seconds), and annealing/extension (58° C, 1 minutes).

Results

Patient 1

A 45-year-old woman who had enjoyed good health before her illness presented with a fever that had begun 4 days prior to admission. Initial investigations showed left upper zone consolidation (chest radiograph) and lymphopenia (peripheral blood examination). The patient failed to respond to levofloxacin with subsequent radiographs, showing progressive involvement of both lower zones. Oral ribavirin and Kaletra were initiated on day 8 after onset of symptoms. In view of persistent fever and increased oxygen demand, pulse methylprednisolone 1 g daily was prescribed for 3 days on day 14. By day 17, the patient's alanine aminotransferase (ALT) level became elevated to 196 IU/L and her albumin level dropped to 27 g/L; bilirubin and coagulation profiles were normal. She did not have a rash, abdominal pain, or jaundice. Her renal function tests and amylase and creatine phosphokinase levels were normal. Lactic acidosis was absent. Despite withdrawal of antivirals on day 22, ALT peaked on day 28 at 493 IU/L (Fig. 1A).

Liver biopsy on day 31 showed mild lobular activities with occasional acidophilic bodies and prominent Kupffer cells. The portal tract was mildly inflamed with lymphocytic infiltration (Fig. 2A). Hepatocytes showed

focal balloon degeneration (Fig. 2B). The mitotic activities were brisk; the mitotic index was 2.1% (Fig. 3). There was no piecemeal necrosis, eosinophilic infiltration, granuloma, cholestasis, fibrosis, steatosis, or fibrin deposition. Immunostaining for CMV was negative. Immunohistochemical study using Ki-67 stain showed numerous hepatocytes in the replicative phase, and the Ki-67 proliferative index was 11.4% (Fig. 4). No abnormal mitosis was noted. Electron microscopy showed a few laminated myelin bodies in the cytoplasm of hepatocytes and Kupffer cells. Microvesicular or macrovesicular fat was minimal. Neither viral particles nor giant mitochondria were seen. RT-PCR for SARS-CoV was positive in liver tissue (Fig. 5A) but not in the serum (Fig. 5B).

The patient's liver function improved gradually, with ALT decreasing to less than 200 IU/L on day 37 upon discharge. She experienced a full recovery, and a liver function test was normal 3 months after discharge. Convalescent serum showed elevation of antibodies to the coronavirus with a titer of 1 in 800.

Patient 2

A 25-year-old woman presented with intermittent fever after contact with a SARS patient in a hospital. Serial chest radiographs were normal. Routine microbiologic and virologic investigations were negative. The patient developed lymphopenia on day 12; on day 14, high-resolution CT of the thorax showed right lower lobe consolidation over posterior retrocardiac segments. RT-PCR for coronavirus was positive in stool specimens on day 16. Ribavirin and Kaletra were started on the same day. On day 21, the patient still had a persistent fever, and high-resolution CT showed increased involvement over both lung fields. Her ALT had elevated to 475 IU/L and her albumin dropped to 27 g/L; liver function subsequently improved (Fig. 1B). Ribavirin and Kaletra were stopped on day 24. Convalescent serum showed elevated antibod-

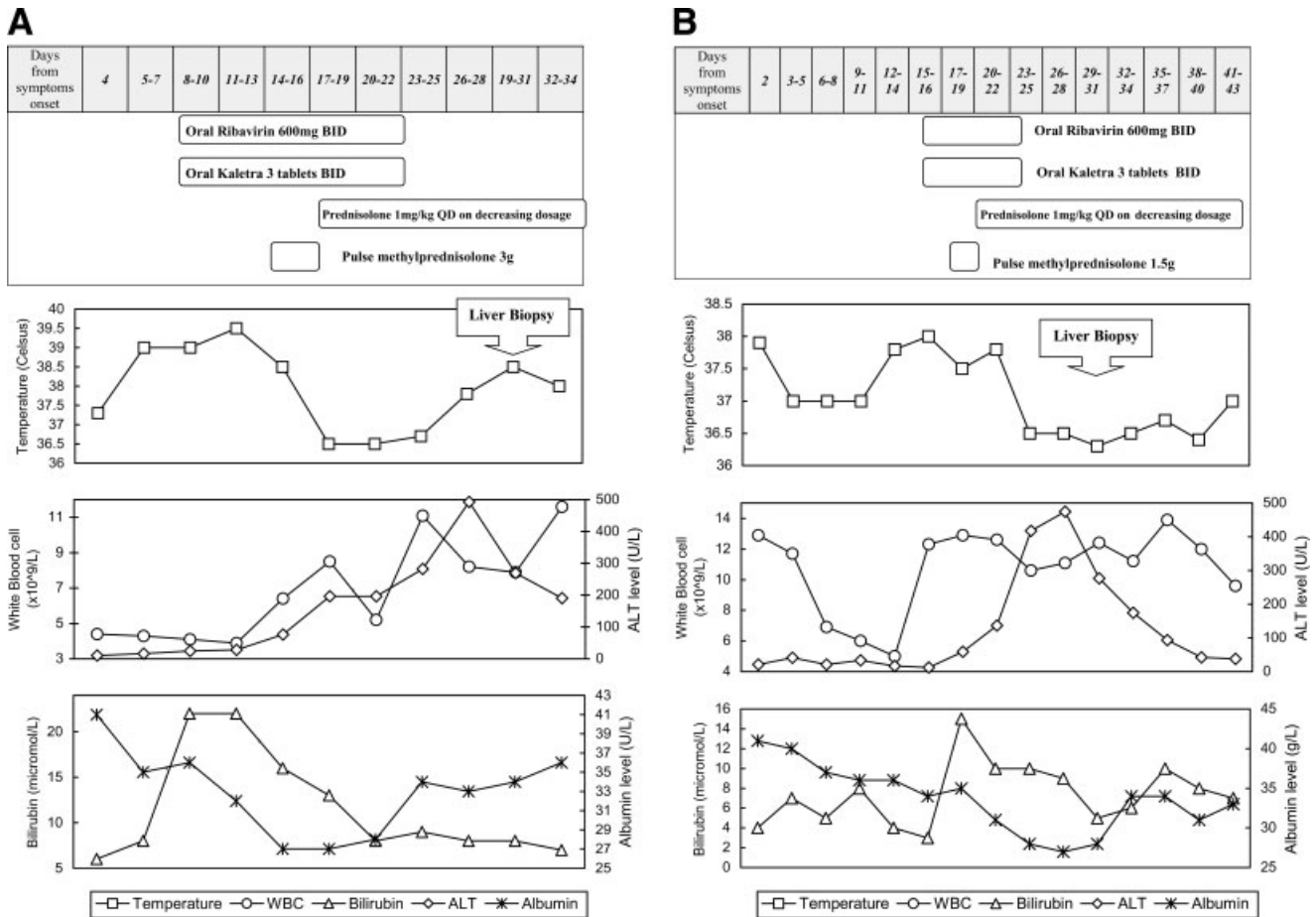


Fig. 1. Temperature, ALT level, white blood cell counts, and treatment of patients 1 (A), 2 (B), and 3 (C).

ies to the coronavirus with a titer of 1 in 400. She was asymptomatic, and her liver function test was normal 3 months after discharge.

Liver biopsy on day 29 showed similar histology to the first patient with mild portal and lobular activity (Fig. 2C) and occasional acidophilic bodies. Prominent mitotic figures were seen in the hepatocytes. The mitotic index was 0.5%. The portal tracts were mildly inflamed. No piecemeal necrosis, steatosis, eosinophilic infiltration, or cholestasis was seen. RT-PCR for coronavirus was positive in the liver tissue (Fig. 5A) but not in the serum (Fig. 5B). The Ki-67 proliferative index was 5.6%. Electron microscopy showed a small number of elongated mitochondria (Fig. 6A) and myelin bodies in hepatocytes. No giant mitochondria, micro- or macro-vesicular steatosis, or viral particles were observed.

Patient 3

A 34-year-old woman presented with fever and cough for 4 days. An initial chest radiograph showed bilateral lower zone consolidation. RT-PCR for coronavirus on nasopharyngeal aspirate was positive. Ribavirin and Kale-

tra were started on day 7 after onset of symptoms when fever persisted despite antibiotics. On day 10, the patient's ALT rose to 399 IU/L and her bilirubin level increased from 6 mmol/L to 21 mmol/L. Pulse methylprednisolone was given on the same day for persistent fever and increased dyspnea. On day 13, the patient improved clinically with resolution of radiographic abnormalities, but her ALT further increased to 941 IU/L. The antivirals were withdrawn. Liver function tests returned to normal on day 26 (Fig. 1C). Both acute and convalescent sera were negative for SARS-associated coronavirus immunoglobulin G.

Liver biopsy on day 14 showed mild to moderate portal and lobular inflammation with predominant lymphocytic infiltration and scattered neutrophils (Fig. 2D). Some hepatocytes showed focal and mild ballooning. The mitotic index was less than 0.1%. A few acidophilic bodies with prominent Kupffer cells were seen. No piecemeal necrosis, steatosis, eosinophilic infiltration, fibrin deposition, or fibrosis was seen. The Ki-67 proliferative index was 0.5%. RT-PCR for coronavirus was positive in liver

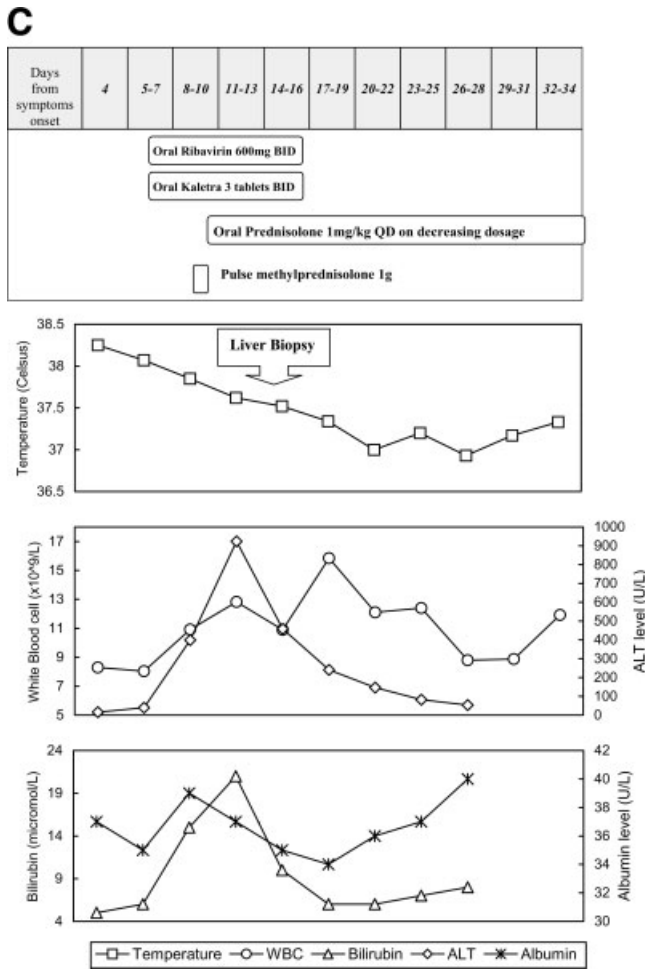


Fig. 1 (Cont'd.)

tissue (Fig. 5A) but not in the serum (Fig. 5B). A few mitotic figures of hepatocytes were identified in the semi-thin section of the electron microscopy block (Fig. 6B). A few lipid droplets were seen in other hepatocytes, but no macro- or micro- vesicular steatosis was observed. Some mitochondria were elongated, but no giant mitochondria were identified. Some Kupffer cells contained lysosomes.

Discussion

In March 2003, a novel coronavirus, SARS-CoV, was discovered to be the causative agent of SARS. The complete genome of SARS-CoV has been sequenced. Phylogenetic analyses and sequence comparisons show that it is not closely related to other known coronaviruses, including two human coronaviruses, HCoV-OC43 and HCoV-229E.^{10,11} Disease spectrum related to this novel coronavirus and its pathogenesis have yet to be explored. Other members of the genus Coronavirus (*e.g.*, mouse hepatitis virus, which is a group 2 coronavirus) can cause liver damage ranging from minimal changes to fulminant hepatitis.¹²⁻¹⁵ The spike protein found on the virion en-

velope and on the plasma membrane of infected cells is responsible for attachment to viral receptor and virus-cell fusion during viral entry and for cell-to-cell fusion during the latter stages of the infection.^{16,17} Studies of mouse hepatitis virus showed that the spike gene determined the viral load in the liver and that the amount of antigen staining and necrosis in the liver correlated with the viral load. Mutation in the spike gene might abbreviate the severity of hepatitis.¹⁸ Pairwise amino acid identity between SARS-coronavirus and other known coronaviruses was less than 30%,¹¹ hence the hepatotropism of this novel coronavirus is unpredictable.

Liver impairment occurs commonly among patients with SARS.^{2,4,5} Our patients have fulfilled the WHO case definition of clinical SARS. The diagnosis was supported by laboratory tests, including (1) a fourfold or greater rise in antibody titer between acute and convalescent phase sera tested in parallel in patients 1 and 2 and (2) PCR positive for SARS-CoV in a stool specimen of patient 2 and nasopharyngeal aspirate of patient 3, respectively. In our three SARS patients with moderate to marked elevation of ALT, prominent mitoses, acidophilic bodies, Kupffer cells, and mild to moderate lobular inflammation were the common histologic features. All of our patients showed positive RT-PCR for SARS-CoV in liver tissue but not in the sera, suggesting that the virus was localized in liver. Indeed, SARS-CoV is detectable in less than 50% of sera of SARS patients beyond 14 days after fever onset.¹⁹ Because ribavirin and Kaletra were given to all three patients prior to liver biopsy, viral replication might possibly be suppressed and hence no virus could be identified by electron microscopy. Alternatively, the viral load in liver may be so low that it would be difficult to be observed ultrastructurally. The only report of liver histology in SARS (other than the present study) was an autopsy showing microvesicular fatty change, focal hemorrhages, and hepatocyte necrosis with scattered acidophilic bodies in liver, but no viral inclusions were observed.²⁰ Because that patient developed respiratory failure and multi-organ failure before death, the changes in liver histology might not be solely due to SARS-CoV infection.

The most remarkable finding in our liver histology was the conspicuous mitoses, which were readily seen by both light and electron microscopy. Immunohistochemical study using Ki-67 stain showed that hepatocytes were highly replicative. Ki-67 proliferative index has also been reported as 0.4% to 1% in chronic active hepatitis C,^{8,21,22} but the index for acute viral hepatitis remains unknown. However, hepatocytes in the mitotic phase are uncommonly seen even in acute or chronic hepatitis and liver cirrhosis even when regeneration takes place rapidly.²³ The finding of conspicuous mitoses in our patients

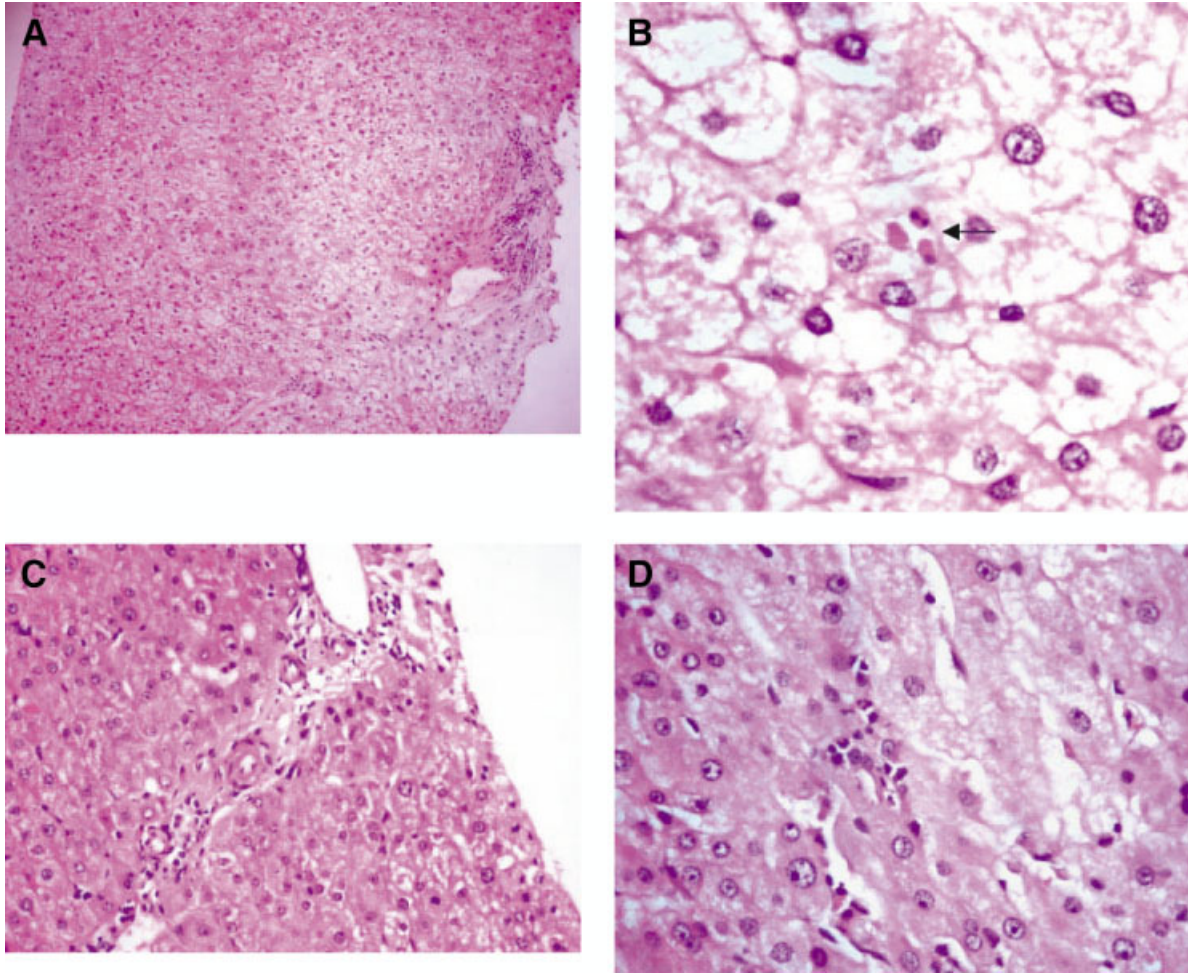


Fig. 2. (A) Histologic section of the liver showing mild portal lymphocytic infiltration and relatively sparse lobular inflammation in patient 1 (Hematoxyline & Eosin $\times 100$). (B) Prominent balloon degeneration of hepatocytes with focal collection of acidophilic bodies (**arrow**) in patient 1 (Hematoxyline & Eosin $\times 400$). (C) Mild portal inflammation in patient 2 (Hematoxyline & Eosin $\times 200$). (D) Lobular activity with focal neutrophilic infiltration in patient 3 (Hematoxyline & Eosin, $\times 400$).

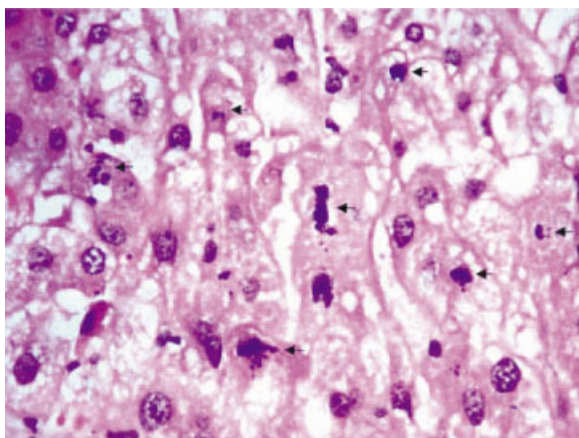


Fig. 3. Extremely brisk mitotic activities (**arrows**) among the hepatocytes in patient 1 (Hematoxyline & Eosin $\times 400$).

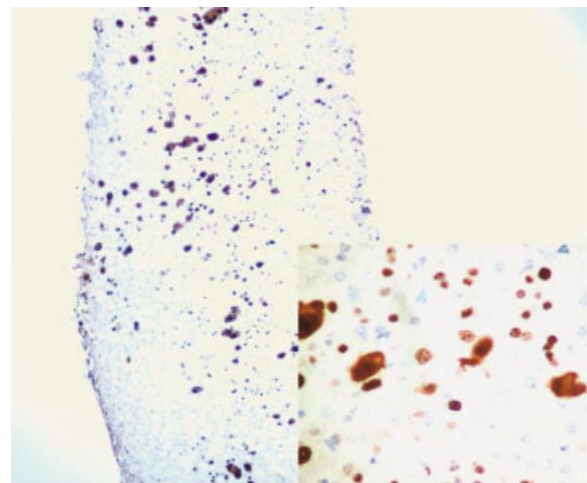


Fig. 4. Immunohistochemical staining for Ki-67 showing marked increase in hepatocyte labeling in patient 1 ($\times 100$; inset $\times 400$).

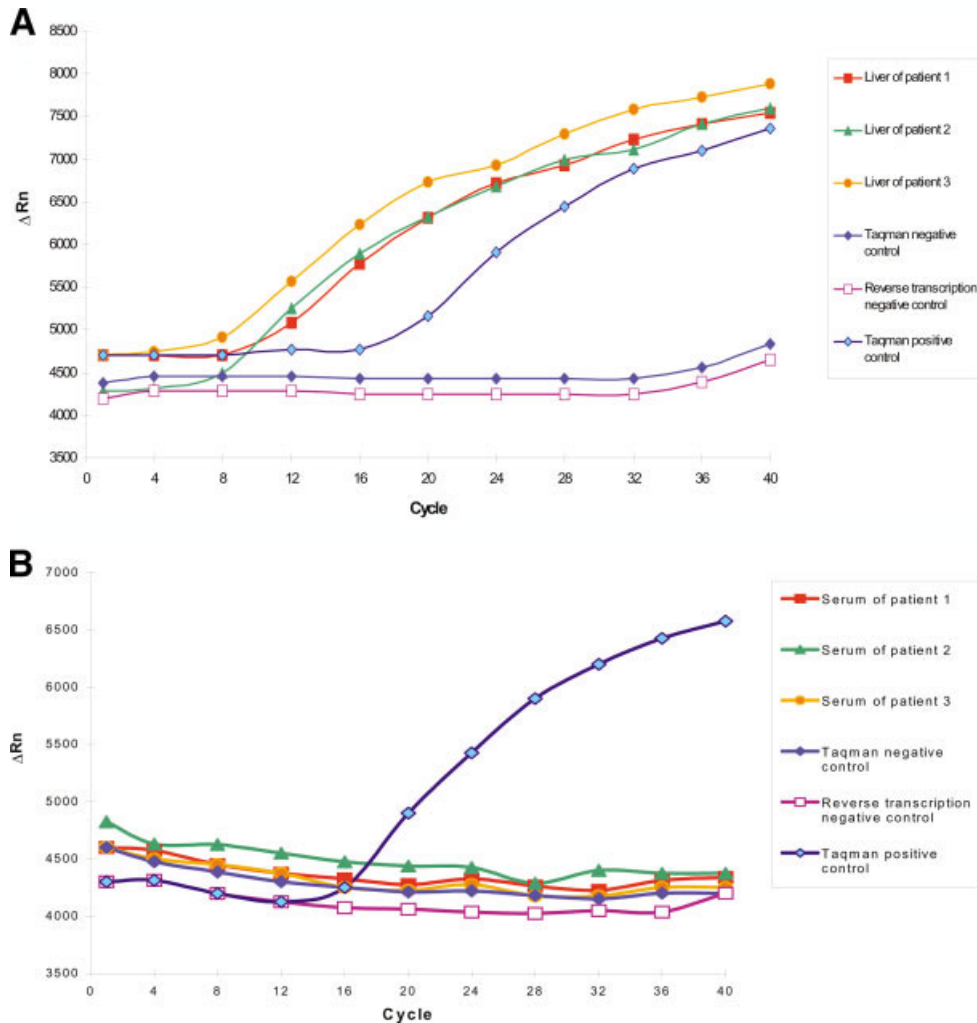


Fig. 5. (A) Liver tissues of all three patients showing positive results for SARS-CoV obtained with real-time PCR as detected by the ABI Prism 7700 Sequence Detector. (B) Sera of all three patients showing negative results for SARS-CoV obtained with real-time PCR as detected by the ABI Prism 7700 Sequence Detector.

appears out of proportion to the extent of liver cell damage as assessed biochemically or histologically. The possibility of cell cycle disruption caused by coronavirus should be considered. Studies of transmissible gastroenteritis virus (a group 1 coronavirus) and mouse hepatitis virus showed that nucleolar localization of nucleoprotein (N protein) is a common feature of the coronavirus family, and about 30% of Vero cells transfected with the nucleoprotein appear to undergo cell division.²⁴ This observation has also been reported in the avian infectious bronchitis virus (a group 3 coronavirus).²⁵ A delay in mitosis or inhibition of cytokinesis could lead to an accumulation of cells in the M phase of the cell cycle and hence the appearance that a significant number of cells undergo cell division. Unlike patients 1 and 2, patient 3 had negative serology for SARS-CoV despite repeatedly positive RT-PCR results on nasal and throat swabs and liver tissue. The lack of immunoglobulin G seroconversion has been described in up to 7% of patients with SARS.⁷ The liver biopsy of this patient also showed higher lobular activities

and less prominent mitotic figures, which might represent another spectrum of disease as a result of different host response to the virus.

Other common pathologic features among the three liver specimens were presence of acidophilic bodies, ballooning of hepatocytes, and mild to moderate lobular activities, which are similar to the hepatic pathology of mouse hepatitis virus in mice.²⁶ The findings suggest that the liver damage due to SARS-coronavirus is mainly mediated by apoptosis. Studies show that some coronaviruses exert extensive cytopathic effect through the induction of apoptosis of their host cells by caspase activation.^{27,28} Mouse hepatitis virus can also activate the immune coagulation system by the *fgl2* gene, which encodes a specific prothrombinase. It induces macrophage procoagulant activity,²⁹ which in turn leads to fibrin deposition on the endothelium of intrahepatic veins and hepatic sinusoids resulting in confluent hepatocellular necrosis. However, our specimens did not show any sinusoidal dilatation or fibrin deposition on the hepatic veins.

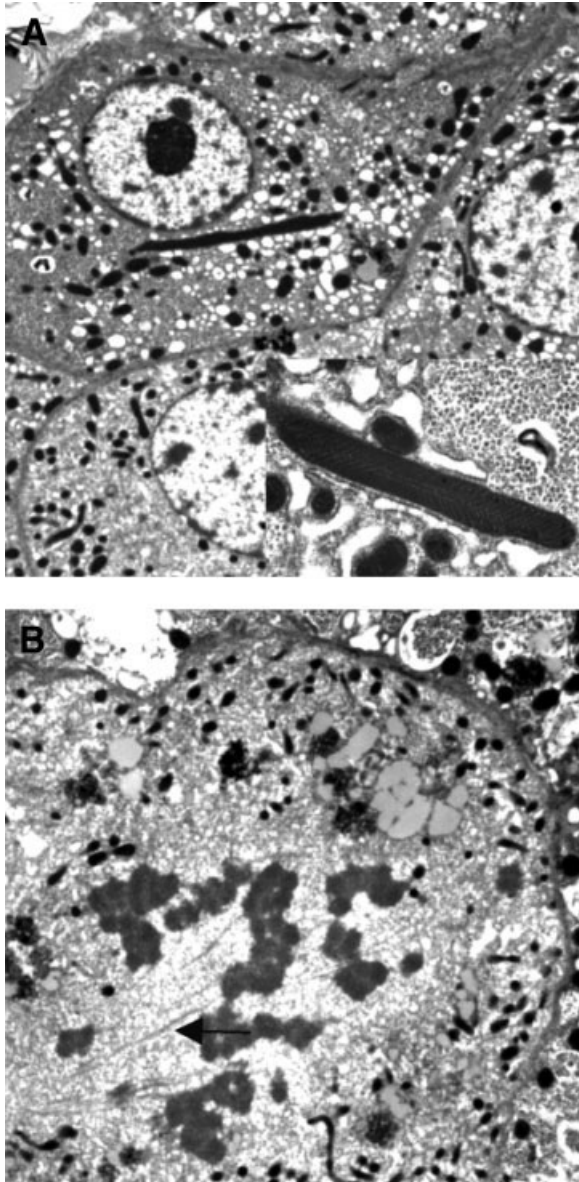


Fig. 6. (A) In patient 2, mitochondria are largely normal ultrastructurally, with occasional ones appearing elongated (Transmission electron microscopy [TEM] $\times 3000$; inset $\times 35000$). (B) Electron microscopy showing a hepatocyte in mitosis with disappearance of nuclear membrane and spindle formation (**arrow**) in patient 3 (TEM $\times 5000$).

On the other hand, fibrin thrombi and intimal swelling of pulmonary vessels have been reported among patients with SARS.³⁰

An alternative explanation of the liver impairment in SARS patients is hepatotoxicity due to antiviral treatment. Kaletra has been used for the treatment of SARS in more than 100 patients in Hong Kong. Preliminary results show that 30-day mortality and intubation rates are lower in the Kaletra-treated group compared with patients treated with ribavirin.³¹ Elevation in ALT greater than fivefold the upper limit of normal has been reported

in 3% to 11% of patients taking Kaletra.³² Ribavirin also increases mitochondrial toxicity in HIV-infected patients treated with protease inhibitors.^{33,34} However, we do not favor this possibility, because hepatotoxicity usually develops only after long-term use of antiviral agents. Furthermore, our patients had no pancreatitis, myopathy, lactic acidosis, or other clinical features suggestive of mitochondrial toxicity. Occasionally, hepatotoxicity may occur in the first few weeks after initiating antiviral therapy; this is typically related to immune-mediated hypersensitivity and generally occurs in conjunction with allergic reactions such as fever and rash.³⁵ However, our patients had no such clinical features, and their liver biopsies did not show any eosinophilia, giant mitochondria, or microvesicular steatosis suggestive of drug toxicity.^{36–39} Furthermore, there is no consistent temporal relationship between the antiviral treatment and liver function impairment. In primary human hepatocytes, ribavirin can also inhibit cell proliferation induced by mitogenic factors by way of a delayed progression to the S phase of the cell cycle.⁴⁰ However, liver histology of patients with chronic hepatitis C does not show any features of cell cycle arrest after ribavirin monotherapy.^{41,42} Further studies are warranted to determine whether or not SARS-CoV infection, like chronic hepatitis B and C virus infection,^{43–45} may increase the hepatotoxicity of the antivirals.

In conclusion, SARS-CoV can infect livers leading to mild to moderate lobular inflammation and apoptosis. The presence of prominent mitoses among hepatocytes possibly due to hyperproliferative state and cell cycle arrest is a cardinal feature of liver pathology in SARS. With a better knowledge of the pathogenesis of SARS-CoV infection, including the possible viral replication in hepatocytes, specific therapy may be targeted to reduce the viral replication and modify the clinical course of the disease.

References

1. Holmes KV, Lai MMC. Coronaviridae and their replication. In: Fields B, Knipe D, Howley P, eds. *Fields virology*. 3rd edition. Philadelphia: Lippincott-Raven, 1996:1075.
2. Peiris JSM, Lai ST, Poon LLM, Guan Y, Yam LYC, Lim W, Nicholls, et al. Coronavirus as a possible cause of severe acute respiratory syndrome. *Lancet* 2003;361:1319–1325.
3. Drosten C, Gunther S, Preiser W, van der Werf S, Brodt HR, Becker S, Rabenau H, et al. Identification of a novel coronavirus in patients with severe acute respiratory syndrome. *N Engl J Med* 2003;348:1967–1976.
4. Lee N, Hui D, Wu A, Chan P, Cameron P, Joynt GM, Ahuja A, et al. A major outbreak of severe acute respiratory syndrome in Hong Kong. *N Engl J Med* 2003;348:1986–1994.
5. Tsang KW, Ho PL, Ooi GC, Yee WK, Wang T, Chan-Yeung M, Lam WK, et al. A cluster of cases of severe acute respiratory syndrome in Hong Kong. *N Engl J Med* 2003;348:1977–1985.
6. WHO. Severe acute respiratory syndrome (SARS). *Wkly Epidemiol Rec* 2003;78:81–83.

7. Peiris JSM, Chu CM, Cheng VCC, Chan KS, Hung IFN, Poon LLM, Law KI, et al. Clinical progression and viral load in a community outbreak of coronavirus-associated SARS pneumonia: a prospective study. *Lancet* 2003;361:1767–1772.
8. Kaita KDE, Pettigrew N, Minuk GY. Hepatic regeneration in humans with various liver disease as assessed by Ki-67 staining of formalin-fixed paraffin-embedded liver tissue. *Liver* 1997;17:13–16.
9. Lau LT, Wang CG, Yu CH. Enhanced detection of the coronavirus associated with severe acute respiratory syndrome (SARS). Abstract presented at the ASEAN, China, Japan, and ROK (10+3) High-Level Symposium on Severe Acute Respiratory Syndrome (SARS) 2003, June 3–4, Beijing, China, 2003. p 31–32.
10. Marra MA, Jones SJ, Astell CR, Holt RA, Wilson AB, Butterfield YSN, Khattra J, et al. The genome sequence of the SARS-associated coronavirus. *Science* 2003;300:1399–1404.
11. Rota PA, Oberste MS, Monroe SS, Nix WA, Campagnoli R, Icenogle JP, Penaranda S, et al. Characterization of a novel coronavirus associated with severe acute respiratory syndrome. *Science* 2003;300:1394–1399.
12. Ning Q, Liu M, Kongkham P, Lai MM, Marsden PA, Tseng J, Pereira B, et al. The nucleocapsid protein of murine hepatitis virus type 3 induces transcription of the novel *fgl2* prothrombinase gene. *J Biol Chem* 1999;274:9930–9936.
13. Hirano N, Murakami T, Taguchi F, Fujiwara K, Matumoto M. Comparison of mouse hepatitis virus strains for pathogenicity in weanling mice infected by various routes. *Arch Virol* 1981;70:69–73.
14. Knobler RL, Haspel MV, Oldstone MB. Mouse hepatitis virus type 4 (JHM strains) induced fatal central nervous system disease: genetic control and murine neuron as the susceptible site of disease. *J Exp Med* 1981;153:832–843.
15. Lavi ED, Gilden H, Wroblewska Z, Rorke LB, Weiss SR. Experimental demyelination produced by the A59 strain of mouse hepatitis virus. *Neurology* 1984;34:597–603.
16. Gallagher TM. Murine coronavirus spike glycoprotein: receptor binding and membrane fusion activities. *Adv Exp Med Biol* 2001;494:183–192.
17. Gallagher TM, Buchmeier MJ. Coronavirus spike proteins in viral entry and pathogenesis. *Virology* 2001;279:371–374.
18. Navas S, Seo SH, Chua MM, Sarma JD, Lavi E, Hingley ST, Weiss SR. Murine coronavirus spike protein determines the ability of the virus to replicate in the liver and cause hepatitis. *J Virol* 2001;75:2452–2457.
19. Ng EKO, Hui DS, Chan AKC, Hung ECW, Chiu RWK, Lee N, Wu A, et al. Quantitative analysis and prognostic implication of SARS-coronavirus RNA in the plasma and serum of patients with severe acute respiratory syndrome. *Clin Chem* 2003;49:1976–1980.
20. Poutanen SM, Low DE, Henry B, Finkelstein S, Rose D, Green K, Tellier R, et al. Identification of severe acute respiratory syndrome in Canada. *N Engl J Med* 2003;348:1995–2005.
21. Kronenberger B, Ruster B, Lee JH, Sarrazin C, Roth WK, Herrmann G, Zeuzem S. Hepatocellular proliferation in patients with chronic hepatitis C and persistently normal or abnormal aminotransferase level. *J Hepatol* 2000;33:640–647.
22. Hussein O, Szvalb S, Akker-Berman LMV, Assy N. Liver regeneration is not altered in patients with nonalcoholic steatohepatitis (NASH) when compared to chronic hepatitis C infection with similar grade of inflammation. *Dig Dis Sci* 2002;47:1926–1931.
23. Wright N, Alison M. The liver. In: Wright N, Alison M, eds. *The Biology Epithelial Cell Populations Volume 2*. Oxford: University Press, 1984: 880–956.
24. Wurm T, Chen H, Hodgson T, Britton P, Brooks G, Hiscox JA. Localization to the nucleolus is a common feature of coronavirus nucleoproteins, and the protein may disrupt host cell division. *J Virol* 2001;75:9345–9356.
25. Hiscox JA, Wurm T, Wilson L, Britton P, Cavanagh D, Brooks G. The coronavirus infectious bronchitis virus nucleoprotein localizes to the nucleolus. *J Virol* 2001;75:506–512.
26. Huang DS, Emancipator SN, Fletcher DR, Lamm ME, Mazanec MB. Hepatic pathology resulting from mouse hepatitis virus S infection in severe combined immunodeficiency mice. *Lab Anim Sci* 1996;42:167–173.
27. Liu C, Xu HY, Liu DX. Induction of caspase-dependent apoptosis in cultured cells by the avian coronavirus infectious bronchitis virus. *J Virol* 2001;75:6402–6409.
28. Eleouet JF, Slee EA, Saurini F, Castagne N, Poncet D, Garrido C, Solary E, et al. The viral nucleocapsid protein of transmissible gastroenteritis coronavirus (TGEV) is cleaved by caspase-6 and -7 during TGEV-induced apoptosis. *J Virol* 2000;74:3975–3983.
29. Ding JW, Ning Q, Liu MF, Lai A, Leibowitz J, Peltekian KM, Cole EH, et al. Fulminant hepatic failure in murine hepatitis virus strain 3 infection: tissue-specific expression of a novel *fgl2* prothrombinase. *J Virol* 1997;71:9223–9230.
30. Nicholls JM, Poon LLM, Lee KC, Ng WF, Lai ST, Leung CY, Chu CM, et al. Lung pathology of fatal severe acute respiratory syndrome. *Lancet* 2003;361:1773–1778.
31. Chu CM. Treatment-Kaletra. Abstract Presented at the SARS Clinical Management Workshop. June 13–14, 2003, Hong Kong, China.
32. Corbett AH, Lim ML, Kashuba DM. Kaletra (lopinavir/ritonavir). *Ann Pharmacother* 2002;36:1193–1203.
33. Lafeuillade A, Hittinger G, Chadapaud S. Increased mitochondrial toxicity with ribavirin in HIV/HCV coinfection. *Lancet* 2001;357:280–281.
34. Salmon-Ceron D, Chauvelot-Moachon L, Abad S, Silbermann B, Sogni P. Mitochondrial toxic effects and ribavirin. *Lancet* 2001;357:1803.
35. Soriano V. Liver disease in HIV: an update. *PRN Notebook* 2002;7:10–15.
36. Benveniste O, Longuet P, Duval X, Moing VL, Lepout C, Vilde JL. Two episodes of acute renal failure, rhabdomyolysis, and severe hepatitis in an AIDS patient successively treated with ritonavir and indinavir. *Clin Infect Dis* 1999;28:1180–1181.
37. Odile P, Olivier R, Jean C. Hepatotoxicity associated with ritonavir. *Ann Intern Med* 1998;129:670–671.
38. Sagir A, Wettstein M, Oette M, Erhardt A, Haussinger D. Budesonide-induced acute hepatitis in an HIV-positive patient with ritonavir as a co-medication. *AIDS* 2002;16:1191–1192.
39. Juzo M, Kengo G, Masami Y. Severe hepatitis in patients with AIDS and haemophilia B treated with indinavir. *Lancet* 1997;350:364.
40. Ilyin GP, Langouet S, Rissel M, Delcros JG, Guillouzo A, Guguen-Guilouzo C. Ribavirin inhibits protein synthesis and cell proliferation induced by mitogenic factors in primary human and rat hepatocytes. *HEPATOLOGY* 1998;27:1687–1694.
41. Hoofnagle JH, Lau D, Conjeevaram H, Kleiner D, Di Bisceglie AM. Prolonged therapy of chronic hepatitis C with ribavirin. *J Viral Hepat* 1996;3:247–252.
42. Dusheiko G, Main J, Thomas H, Reichard O, Lee C, Dhillon A, Rassam S, et al. Ribavirin treatment for patients with chronic hepatitis C: results of a placebo-controlled study. *J Hepatol* 1996;25:591–598.
43. Wit FW, Weverling GJ, Weel J, Jurriaans S, Lange JM. Incidence of and risk factors for severe hepatotoxicity associated with antiretroviral combination therapy. *J Infect Dis* 2002;186:23–31.
44. Gisolf EH, Dreezen C, Danner SA, Weel JL, Weverling GJ, Prometheus Study Group. Risk factors for hepatotoxicity in HIV-1-infected patients receiving ritonavir and saquinavir with or without stavudine. *Clin Infect Dis* 2000;31:1234–1239.
45. Marianne S, Stephanie V, Valentina D, Catherine M, Michell D, Patrice C, Noelle B, et al. Severe hepatic cytolysis: incidence and risk factors in patients treated by antiretroviral combinations Aquitaine cohort, France, 1996–1998. *AIDS* 1999;13:115–151.